A fiber optic probe design to measure depth-limited optical properties *in-vivo* with Low-coherence Enhanced Backscattering (LEBS) Spectroscopy

Nikhil N. Mutyal, Andrew Radosevich, Bradley Gould, Jeremy D. Rogers, Andrew Gomes, Vladimir Turzhitsky, and Vadim Backman*

[1]*Department of Biomedical Engineering, Northwestern University, 2145 Sheridan Road, Evanston IL 60208, USA*
**v-backman@northwestern.edu*

Abstract: Low-coherence enhanced backscattering (LEBS) spectroscopy is an angular resolved backscattering technique that is sensitive to sub-diffusion light transport length scales in which information about scattering phase function is preserved. Our group has shown the ability to measure the spatial backscattering impulse response function along with depth-selective optical properties in tissue *ex-vivo* using LEBS. Here we report the design and implementation of a lens-free fiber optic LEBS probe capable of providing depth-limited measurements of the reduced scattering coefficient *in-vivo*. Experimental measurements combined with Monte Carlo simulation of scattering phantoms consisting of polystyrene microspheres in water are used to validate the performance of the probe. Additionally, depth-limited capabilities are demonstrated using Monte Carlo modeling and experimental measurements from a two-layered phantom.

OCIS codes: (170.6510) Spectroscopy, tissue diagnostics; (290.1350) Backscattering, (060.2310) Fiber optics.

References and links

1. G. A. Wagnières, W. M. Star, and B. C. Wilson, "In vivo fluorescence spectroscopy and imaging for oncological applications," Photochem. Photobiol. **68**(5), 603–632 (1998).
2. A. Richter, K. Yang, F. Richter, H. T. Lynch, and M. Lipkin, "Morphological and morphometric measurements in colorectal mucosa of subjects at increased risk for colonic neoplasia," Cancer Lett. **74**(1-2), 65–68 (1993).
3. C. Booth, G. Brady, and C. S. Potten, "Crowd control in the crypt," Nat. Med. **8**(12), 1360–1361 (2002).
4. R. Barer and S. Joseph, "Refractometry of living cells," J. Microscop. Sci. **s3–95**, 399–423 (1954).
5. J. D. Rogers, I. R. Capoğlu, and V. Backman, "Nonscalar elastic light scattering from continuous random media in the Born approximation," Opt. Lett. **34**(12), 1891–1893 (2009).
6. V. Turzhitsky, A. J. Radosevich, J. D. Rogers, N. N. Mutyal, and V. Backman, "Measurement of optical scattering properties with low-coherence enhanced backscattering spectroscopy," J. Biomed. Opt. **16**(6), 067007 (2011).
7. H. K. Roy, V. Turzhitsky, Y. Kim, M. J. Goldberg, P. Watson, J. D. Rogers, A. J. Gomes, A. Kromine, R. E. Brand, M. Jameel, A. Bogovejic, P. Pradhan, and V. Backman, "Association between rectal optical signatures and colonic neoplasia: potential applications for screening," Cancer Res. **69**(10), 4476–4483 (2009).
8. B. Yu, H. Fu, T. Bydlon, J. E. Bender, and N. Ramanujam, "Diffuse reflectance spectroscopy with a self-calibrating fiber optic probe," Opt. Lett. **33**(16), 1783–1785 (2008).
9. T. Papaioannou, N. W. Preyer, Q. Fang, A. Brightwell, M. Carnohan, G. Cottone, R. Ross, L. R. Jones, and L. Marcu, "Effects of fiber-optic probe design and probe-to-target distance on diffuse reflectance measurements of turbid media: an experimental and computational study at 337 nm," Appl. Opt. **43**(14), 2846–2860 (2004).
10. R. A. Schwarz, D. Arifler, S. K. Chang, I. Pavlova, I. A. Hussain, V. Mack, B. Knight, R. Richards-Kortum, and A. M. Gillenwater, "Ball lens coupled fiber-optic probe for depth-resolved spectroscopy of epithelial tissue," Opt. Lett. **30**(10), 1159–1161 (2005).
11. A. Amelink, H. J. C. M. Sterenborg, M. P. L. Bard, and S. A. Burgers, "*In vivo* measurement of the local optical properties of tissue by use of differential path-length spectroscopy," Opt. Lett. **29**(10), 1087–1089 (2004).

#169818 - $15.00 USD Received 6 Jun 2012; revised 3 Aug 2012; accepted 6 Aug 2012; published 13 Aug 2012

12. A. Dhar, K. S. Johnson, M. R. Novelli, S. G. Bown, I. J. Bigio, L. B. Lovat, and S. L. Bloom, "Elastic scattering spectroscopy for the diagnosis of colonic lesions: initial results of a novel optical biopsy technique," Gastrointest. Endosc. **63**(2), 257–261 (2006).
13. S. P. Lin, L. Wang, S. L. Jacques, and F. K. Tittel, "Measurement of tissue optical properties by the use of oblique-incidence optical fiber reflectometry," Appl. Opt. **36**(1), 136–143 (1997).
14. V. Turzhitsky, N. N. Mutyal, A. J. Radosevich, and V. Backman, "Multiple scattering model for the penetration depth of low-coherence enhanced backscattering," J. Biomed. Opt. **16**(9), 097006 (2011).
15. J. D. Rogers, V. Stoyneva, V. Turzhitsky, N. N. Mutyal, P. Pradhan, I. R. Çapoğlu, and V. Backman, "Alternate formulation of enhanced backscattering as phase conjugation and diffraction: derivation and experimental observation," Opt. Express **19**(13), 11922–11931 (2011).
16. J. D. Rogers, V. Stoyneva, V. Turzhitsky, N. Mutyal, and Y. Ji, H. K. Roy, and V. Backman, "Polarized enhanced backscattering spectroscopy for characterization of biological tissues at sub-diffusion length- scales," IEEE J. Sel. Top. Quantum Electron. (to be published).
17. Y. L. Kim, Y. Liu, V. M. Turzhitsky, R. K. Wali, H. K. Roy, and V. Backman, "Depth-resolved low-coherence enhanced backscattering," Opt. Lett. **30**(7), 741–743 (2005).
18. V. Turzhitsky, J. D. Rogers, N. N. Mutyal, H. K. Roy, and V. Backman, "Characterization of light transport in scattering media at sub-diffusion length scales with Low-coherence Enhanced Backscattering," IEEE J. Sel. Top. Quantum Electron. **16**(3), 619–626 (2010).
19. J. C. Ramella-Roman, S. A. Prahl, and S. L. Jacques, "Three Monte Carlo programs of polarized light transport into scattering media: part II," Opt. Express **13**(25), 10392–10405 (2005).

1. Introduction

Optical spectroscopy is a promising technique for the minimally invasive detection of cancers and precancers [1]. The onset of precancer induces several structural changes in the mucosal morphology [2,3] that result in changes in mass density distribution. According to the Gladstone-Dale eq. (n (Refractive Index) = $n_{water} + \alpha\rho$), where ρ (g/ml) is the concentration of tissue solids (primarily macromolecules) and refractive index increment α ~0.17 to 0.2 ml/g. Thus, changes in the spatial distribution of mass density are directly related to changes in the distribution of refractive index [4]. As a result, these changes in tissue morphology can be readily measured by analyzing the backscattering signal [5]. The statistics (and their alteration in disease) of the spatial distribution of density and the corresponding refractive index can be parameterized by three quantities: 1) the variance of the spatial variations of refractive index Δn^2; 2) the correlation length of refractive index variation l_c; and 3) the shape of the correlation function m [5]. These changes in physical properties lead to alterations in the macroscopic light scattering properties of tissue (e.g. reduced scattering coefficient μ_s* and anisotropy coefficient g) [5–7]. Most precancerous structural changes take place in the top mucosal layer, which causes changes in the light scattering properties of that layer [2,3]. A modality which restricts the depth of interrogation photons to this layer maximizes the sensitivity of the measured optical properties to alterations in disease and provides an optimal diagnostic capability. Hence the measurement of depth-limited optical properties serves as a tool to characterize the structure of any material, and can be diagnostically significant for tissue measurements.

Many techniques such as Diffuse Reflectance Spectroscopy [8–10], Differential Path Length Spectroscopy [11], Elastic Light Scattering Spectroscopy [12], and Oblique-Incidence Optical Fiber Re⟩ectometry [13] provide an excellent ability to measure depth-resolved/limited optical properties of tissue *in-vivo* (μ_s,μ_a). Our group has recently developed Low-Coherence Enhanced Backscattering (LEBS) spectroscopy, which has the additional advantages of sensitivity to sub-diffusion light transport length scales for which information about scattering phase function is preserved along with depth-limited interrogation (superficial depths) [5,6,14]. Enhanced backscattering (EBS) is a result of the constructive interference between photons traveling time-reversed paths in a turbid medium. The EBS phenomenon manifests itself as an enhancement of scattered light intensity in the backward direction with respect to the incident light. The shape of an EBS peak as a function of angle is sensitive to μ_s* and the shape of the phase function [6]. Using an LEBS benchtop system, we have demonstrated that low spatial coherence illumination (coherence length $L_{SC} << l_s^*$, $l_s^* =$

#169818 - $15.00 USD Received 6 Jun 2012; revised 3 Aug 2012; accepted 6 Aug 2012; published 13 Aug 2012

$1/\mu_s'$ - light transport mean free path ~1 mm) facilitates the detection and quantification of this effect in tissue [6,7]. Depth selectivity is achieved by selecting L_{SC}, which acts as a spatial filter limiting the radial displacement of photons that interfere to form the LEBS peak (a smaller L_{SC} rejects the signal from deeper tissue, resulting in a shorter average penetration depth) [14]. In our recent publications we have shown that *ex-vivo* measurement of optical properties by LEBS in rectal mucosal biopsies were able to predict the risk of future neoplasia elsewhere in the colon with 90% accuracy (area under ROC curve) [7]. However, the benchtop system can only be used for *ex-vivo* measurements due to its large size (Fig. 1); hence there is a need to develop a fiber optic probe for *in-vivo* use.

In this manuscript the design, development, and implementation of a lens-free fiber optic probe capable of depth-limited measurements of the reduced scattering coefficient of tissue *in-vivo* is described. The manuscript is organized in the following way: section two describes the LEBS *ex-vivo* observation and the process behind the conversion of the *ex-vivo* system to an *in-vivo* probe. Section three outlines the principles of the observation of LEBS with a fiber optic probe. Section four describes the design and implementation of the fiber optic LEBS probe, while section five demonstrates the measurement of the LEBS signal and verification with phantom and Monte Carlo simulations. Section six demonstrates depth selectivity of measurement with two-layered phantoms and MC simulations, and section seven discusses the novelty and limitation of the fiber optic probe, followed by the conclusion in section eight.

2. LEBS *ex-vivo* experimental observation

The LEBS intensity peak defined by Eq. (1) is the Fourier transform of the spatial backscattering impulse-response function ($P(r)$) multiplied by the spatial coherence function ($C(r)$) [6].

$$I_{LEBS}(\theta) = FT\,[P(r).C(r)] \tag{1}$$

The $C(r)$ (and L_{SC}) can be controlled experimentally, whereas $I_{LEBS}(\theta)$ is recorded by means of a lens projecting the angular distribution of reflected light onto a focal plane as shown in Fig. 1(a) [6,7]. The $P(r)$ at sub-diffusion length scales and the optical and physical properties of tissue can therefore be calculated from Eq. (1) [5,6]. In setup (Fig. 1(a)) the first lens collimates the beam from a broadband light source onto the sample. When the illumination is collimated, the source can be described as being located infinitely far from the sample, and therefore the peak is localized at infinity. The backscattered signal can be collected by another lens and focused onto a CCD by using a beam splitter. The LEBS peak can also be observed in the retro-reflection direction in the plane of the light source if the beam splitter is absent (Fig. 1(a) dotted). Both setups yield identical information, however, and differ only in the number of required optical components. For example, in a setup without a beam splitter one lens is removed and hence the setup is more compact and can be built into a fiber optic probe.

Recently, we reported the implementation of a lens-free benchtop system to measure LEBS [15]. The lens-free assembly works on the principle of phase conjugation, where the light source at a finite distance from the medium produces the peak at a point conjugate to the source.

#169818 - $15.00 USD Received 6 Jun 2012; revised 3 Aug 2012; accepted 6 Aug 2012; published 13 Aug 2012

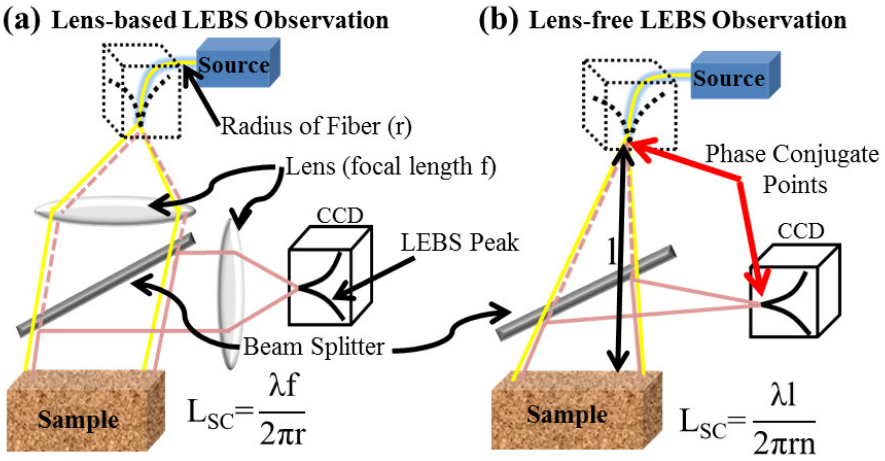

Fig. 1. LEBS peak can be experimentally observed in two ways: (a) lens-based observation and (b) lens-free observation. In lens-based observation the beam of light from a broadband light source is collimated using a lens and relayed to the sample; the backscattered light is then collimated by a lens onto the detector. In lens-free observation the light beam diverges onto the sample; the backscattered diverging beam can then be captured by the detector. The peak can be detected in a separate arm by placement of the beam splitter or in the exact backward direction (probe design) at the light source plane (when a beam splitter is absent).

In this setup (Fig. 1(b)), we can eliminate the use of lenses by employing a diverging illumination beam. The diverging beam illuminates the sample and the backscattered light forms a peak at the point in space conjugate to the source. Like the lens-based LEBS setup, this configuration can be used in two modes: 1) with and 2) without beam splitter. In the lens-free configuration (Fig. 1(b)) we acquire the same LEBS peak as with the lens-based setup [9] (Fig. 1(a)), but have elegantly eliminated all lenses and the beam splitter (which is advantageous for building compact and low-cost fiber optic probes for *in-vivo* applications). Based on this premise we designed and implemented both lens-based and lens-free fiber optic probes to compare their performance and evaluate any advantage of one configuration over the other. The choice of probe configuration is discussed in section 3.

3. LEBS observation with fiber optic probe

The light scattering optical properties of tissue (μ_s*,g & D_f (fractal dimension)) are measured by fitting the LEBS peak to those obtained numerically by Monte Carlo simulations or by using a look-up Table [6]. Translating the entire benchtop assembly (Fig. 1(a,b)) into a fiber optic probe would require sampling the whole 2D plane of the peak via a fiber bundle. This configuration, though theoretically possible, would require several detectors (or a 2D array) and would remain neither compact nor low-cost. However, because unpolarized light gives a symmetrical LEBS peak [16], we hypothesized that information about the reduced scattering coefficient could be obtained solely by detecting the signal from a few backscattering angles within the LEBS intensity cone. Therefore the principle behind this probe is the acquisition of the LEBS signal for three backscattering angles within the LEBS intensity cone with respect to each collection fiber. The choice of three angles is based on the concept that one fiber should measure the incoherent baseline (diffuse background) while the other two measure one backscattering intensity cone each, thus giving one parameter which has information about the LEBS peak. This is achieved by the collinear alignment of four fibers as shown in Fig. 2(a). The collinear fiber assembly is superimposed at the light source plane in setups shown in Fig. 1 (a,b) with the beam splitters eliminated, which results in the formation of the LEBS peak in the retro-reflection direction. The cross section of the probe tip assembly is depicted in Fig. 2(b,c) for the lens-based and lens-free LEBS fiber optic probes, respectively. In each

#169818 - $15.00 USD Received 6 Jun 2012; revised 3 Aug 2012; accepted 6 Aug 2012; published 13 Aug 2012

setup, channel Z is connected to the broadband light source. The LEBS peak forms at the plane of the illumination fiber (dotted line Fig. 2(b and 2c) and is detected by the fiber array (A',A & B) placed collinearly to it. Channels A & A' sample 0.6 ± 0.24 degrees on either side of the peak (red dots depicted in Fig. 2(b and 2c)). Channel B samples 1.18 ± 0.24 degrees, which is approximately the incoherent baseline. Thus, the three LEBS intensities from the backscattering angles in the 2D peak are mapped onto the spectrometer to give the intensity profile in 1D (red dots in Fig. 2b and 2c). The intensities collected by Channels A, A'& B are defined by Eqs. (2) and (3)

$$I_{A,A'}(\Theta = \pm 0.6°, \lambda) = E(\Theta = \pm 0.6°, \lambda) + I_{Diffuse}(\Theta = \pm 0.6°, \lambda) \quad (2)$$

$$I_{B}(\Theta = 1.18°, \lambda) = I_{Diffuse}(\Theta = 1.18°, \lambda) \quad (3)$$

where $I_{Diffuse}(\Theta, \lambda)$ is the diffuse intensity and $E(\Theta, \lambda)$ is the LEBS interference signal denoting a rise above the diffuse baseline ($I_{Diffuse}$) both for certain collection angles Θ. Also since

$$I_{Diffuse}(\Theta = \pm 0.6°, \lambda) \sim I_{Diffuse}(\Theta = 1.18°, \lambda) \quad (4)$$

The LEBS signal (E - rise above diffuse baseline at Θ = ± 0.6°) can be obtained by the subtraction of Eq. (3) from Eq. (2) as given in Eq. (5)

$$E(\Theta = \pm 0.6°, \lambda) = I_{A,A'}(\Theta = \pm 0.6°, \lambda) - I_{B}(\Theta = 1.18°, \lambda) \quad (5)$$

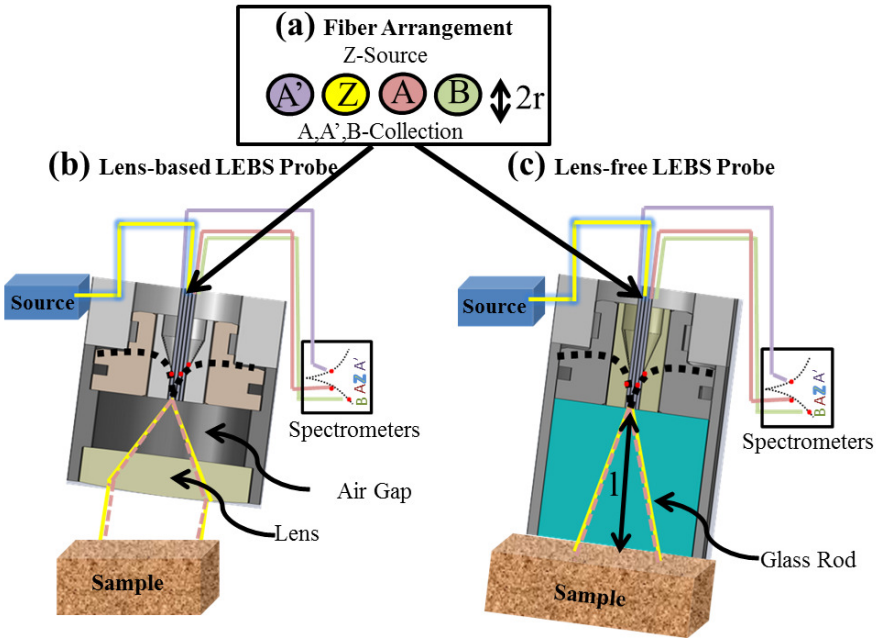

Fig. 2. In order to convert the 2D *ex-vivo* system (Fig. 1) to an *in-vivo* probe, the beam splitter is removed and the peak is detected in retro-reflective direction at the light source plane. The detectors are the fibers in array (Fig. 3 (b). A, A'&B) surrounding the light source fiber (Z) which collect several backscattering angle cones. (b&c) shows the lens-based and lens-free version of the probe assembly.

For example: the 2D LEBS peak from a white reflectance standard obtained from setup (Fig. 1 (a,b)) is shown in Fig. 3(a). When the collinear fiber detection geometry (Fig. 2(a) or 3(b)) is superimposed over the LEBS collection from the 2D peak (Fig. 3(a)), the angular intensity distribution profile (as shown in Fig. 3(c)) is obtained. The intensities are the

#169818 - $15.00 USD Received 6 Jun 2012; revised 3 Aug 2012; accepted 6 Aug 2012; published 13 Aug 2012

specific LEBS backscattering cone intensities captured by the probe collection fibers at particular angles. While Fig. 3(c) shows each collection fiber in 2D, the actual intensity captured through the probe is an average of all pixels. Note that the probe does not collect a signal through channel Z, as it is connected to the light source. Thus the principle of measuring LEBS via a fiber optic probe is based on capturing three intensity values as represented in Fig. 3(c), instead of the whole 2D peak as was the case in *ex-vivo* LEBS observation (Fig. 3(a)).

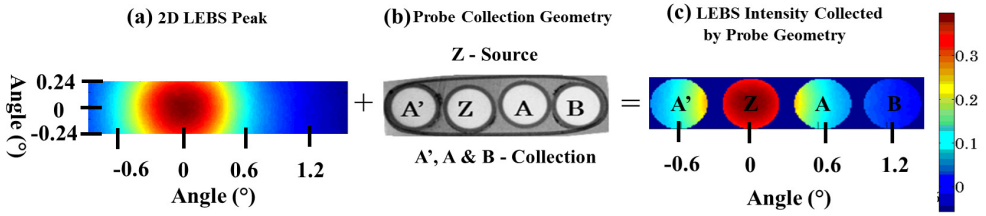

Fig. 3. (a) 2D LEBS peak is shown for white reflectance standard with L_{SC} 27µm at 680nm which is obtained from LEBS ex-vivo system. (b) The front end of the probe is shown, with fiber Z used as illumination and the other three (A', A & B) used as collection. (c) Once the fiber geometry is superimposed on the LEBS 2D peak, the shown profile is obtained

The LEBS peak is formed due to the interference of time-reversed photons above the incoherent (diffuse) baseline as given by Eq. (2) and (3) and represented in Fig. 3(a). We have shown that LEBS intensity at each angle on the LEBS peak is sensitive to various optical properties and represents a particular penetration depth [17]. The 2D *ex-vivo* experimental setup collects the entire peak. The probe design collects backscattering intensity angles at ± 0.6 ± 0.24 (A&A') and 1.18 ± 0.24 (B) degrees (Eq. (2), (3), and (5)), and we hypothesize that this information would be sufficient to experimentally measure the depth-limited reduced scattering coefficient for diagnostics *in-vivo*. To verify this, we modeled the LEBS signal intensities collected via probe geometry with the Mie Monte Carlo (Mie MC) simulation developed by our group [18]. A slab of a medium composed of polystyrene beads in water was used. The code collected only small-angle backscattered rays from 0° to 10° most suitable for modeling backscattering, and the Mie phase function was used in MC to obtain the probability distribution of backscattered light ($P(r)$). The 2D LEBS peaks were obtained by numerically computing the Fourier transform of $P(r)*C(r)$ from Eq. (1). The average LEBS intensities ($E(\Theta, \lambda)$) obtained from the peak simulated by Mie MC were collected at the same angles as the probe detection fibers (± 0.6° ± 0.24 for A & A' & 1.8° ± 0.24 for B) and are shown in Fig. 4(a). There are several items here worth noting: 1) since the LEBS peak is rotationally symmetric for unpolarized illumination, the intensities of fibers A & A' collecting ± 0.6 ± 0.24° are exactly the same; 2) fibers A & A' collecting LEBS intensity near the peak (± 0.6 ± 0.24°) have higher intensities (nearly 3 times) compared to fiber B collecting the incoherent baseline away from the peak (1.18 ± 0.24°), and 3) the intensities are proportional to μ_s* as indicated in our other publications [12]. The implication of these observations is that intensities collected by fiber geometry measure part of the LEBS signal, and these signals are sensitive to optical properties (μ_s* & g).

The novelty of the lens-free fiber optic probe lies in the fact that it is the first observation of LEBS despite the similarity of the probe design to other probes [8–11] (especially ones measuring diffuse reflectance spectroscopy (DRS)). The main difference between this probe and the traditional DRS and Differential Path Length spectroscopy probes is the ability to measure depth-limited optical properties from the low-coherent EBS intensity. In order for the coherent intensity to occur we need to have partial coherence of light (coherence length $L_{SC} << l_s$*), which cannot be attained by any other probe currently developed

#169818 - $15.00 USD Received 6 Jun 2012; revised 3 Aug 2012; accepted 6 Aug 2012; published 13 Aug 2012

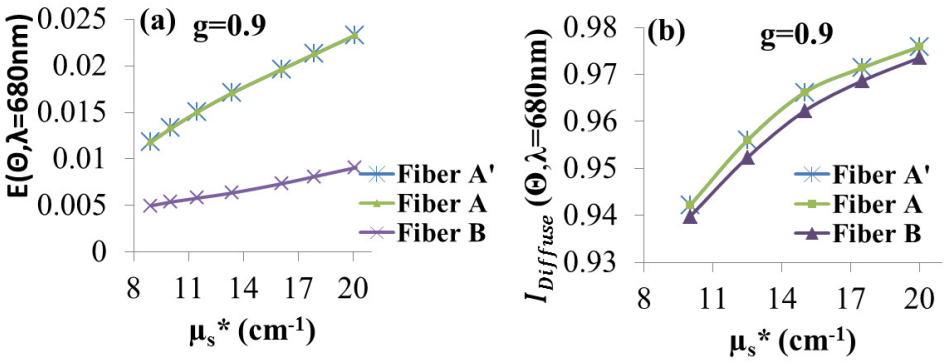

Fig. 4. (a) The LEBS intensities collected by various detection fibers of the probe geometry simulated by MC. The fibers A & A' collect significantly higher (three times) intensity than B due to the presence of an interference signal (LEBS component) (b) The Diffuse Reflectance intensities collected by the same fibers show similar intensities when the interference signal is absent ($L_{SC} = 0$).

due to the large radius of fiber (radius is inversely proportional to L_{sc}). In addition, the fibers need to be placed in very close proximity to detect the enhanced intensity observed at smaller angles. Our probe has overcome both these engineering challenges by 1) employing a fiber with a smaller core, 2) placing fibers in very close proximity, and 3) isolating the interference signal above diffuse intensity (I_A-I_B from Eq. (5)). Notwithstanding these changes, we wanted to demonstrate the distinctive capability of our probe compared to DRS probes.

To illustrate this we modeled the DRS signal of our probe geometry using Monte Carlo (MC) code based on that developed by Ramella-Roman I [19] and simulated the illumination collection geometry of the fiber optic probe to quantify the behavior of the average penetration depth and diffuse reflectance signal in relation to the optical properties of the medium. Unlike the MC described earlier (Fig. 4(a)), this MC did not take into account any interference effect - only diffuse intensity collection from the same geometry. The geometry of the fiber optic probe is shown in Fig. 2 and 3. At the junction of the glass rod and the sample, the incoming light beam has a diameter of ~0.26 cm based on the overall length of the glass rod (l = 9mm) and the numerical aperture (NA) of the illumination fiber (0.22). In the MC code, the initial entry x-y coordinate of a photon into the medium is randomly selected from within this 0.26 cm diameter illumination area. For simplicity, we considered the illumination fiber to be a point source such that the entry angle of a photon can be computed directly from the initial entry x-y coordinate and the length of the glass rod. Light propagation within the medium is determined by the scattering coefficient (μ_s), the absorption coefficient (μ_a), and the properties of the phase function. We employed a Mie phase function for these simulations [18].

The application of this phase function to Monte Carlo has been discussed previously by Radosevich *et al*. [16]. We performed simulations for g = 0.9 and μ_s = [100-200 cm^{-1}]. When a photon reached the junction of the glass rod and the sample, its trajectory was traced to the collection fiber plane at the other end of the glass rod. A photon was considered collected if it intercepted a collection fiber within the NA of the fiber (NA = 0.22). Reflectance intensity was recorded for each collection fiber separately. Boundary reflection between the glass rod (n = 1.52) and the sample (n = 1.33) was handled through Fresnel equations. Ten million photons were tracked for each simulation. The normalized diffuse intensity obtained from these MC simulations is plotted in Fig. 4(b). As expected, when coherence is not present the DR intensities collected by the fibers (A, A'&B) of the probe are very similar, indicating the absence of enhanced backscattering. Also, in the case where coherence in present, as depicted by Eq. (6),

#169818 - $15.00 USD Received 6 Jun 2012; revised 3 Aug 2012; accepted 6 Aug 2012; published 13 Aug 2012

$$\frac{E\ (\Theta = \pm 0.6°, \lambda)}{I_{Diffuse}(\Theta = \pm 0.6°, \lambda) - I_{Diffuse}(\Theta = 1.18°, \lambda)} > 4 \qquad (6)$$

the dominant signal is that of enhanced backscattering. This demonstrates that probes which do not have a condition for finite spatial coherence do not detect enhanced signals (as is detected by our probe geometry (Eqs. (5) and (6)), thus indicating the novelty of design.

We designed both configurations of the fiber optic probe: lens-based and lens-free (Fig. 2) and verified that both measure identical LEBS peaks. The decision to use a lens-free configuration as the preferred design was evaluated on the basis of SNR, ease of manufacture, and cost. We measured the background reflection intensity by pointing the probe at a dark corner of the room and observed that the lens-based probe gave a two-times higher reflection (Fig. 5(a)) as compared to the lens-free configuration. The origin of these reflections is attributed to the presence of an air gap (Fig. 2) between the fibers and the lens versus a refractive index matched glass rod being present in the lens-free configuration. The presence of these reflections lowers the SNR of the lens-based probe. We evaluated the SNR of both probes by measuring I_A-I_B (Eq. (5)) from a white reflectance standard (Spectralon, Labsphere Inc., NH) and observed that the lens-free configuration had four times the SNR as compared to a lens-based probe configuration (Fig. 5(b)). The strong background intensity in the lens-based probe could be reduced by using an index matched media to fill the gap between the fiber and lens or by cleaving the fibers at 8 degrees. However, we found that there are more practical advantages of using a lens-free over a lens-based design such as 1) ease of alignment/manufacture, 2) lower cost, and 3) less maintenance. Therefore we chose the lens-free configuration with no beam splitter (Fig. 1(b) & 2(c)) as the preferred design for an LEBS fiber optic implementation, and will henceforth in this manuscript focus on that configuration.

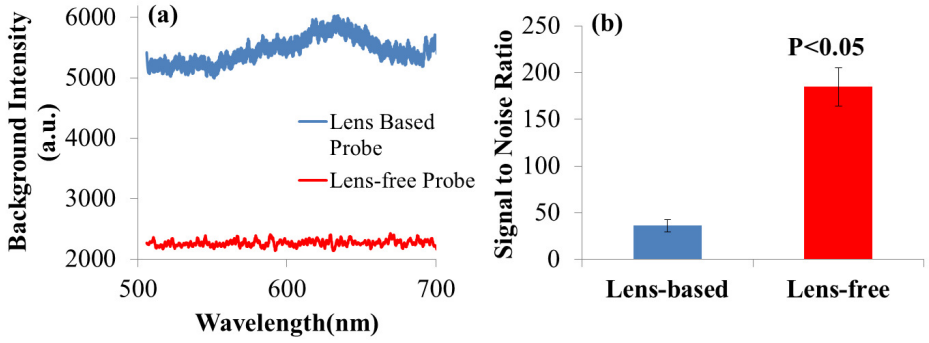

Fig. 5. (a) The background intensity with the probe pointing towards a dark corner is due to reflection at the fiber interface as is shown in the two probe assemblies. In the case of a lens-based LEBS probe the reflections are 2-3 times stronger due to the presence of reflections from the lens as compared to a lens-free LEBS probe, the consequence of which is a higher SNR for a white reflectance standard in the lens-free LEBS probe as depicted in (b).

4. Design and implementation of probe

In order for the probe to be compatible with an endoscopic instrument channel, the outer diameter was restricted to 3.4 mm. The length of the fiber optic probe is 3 meters and the length of the rigid part of the probe is 1.54cm, and we verified that the probe inserted from proximal end of the endoscope via the accessory channel arrives at the distal end (Fig. 6(a)). The beam splitter that separates the illumination (Fig. 1(a and 1b)) from detection angles was eliminated and these two angles were accordingly combined in a compact tubing with an outer diameter of 3.4 ± 0.1 mm (the geometrical arrangement of the illumination and collection fibers as seen from the front is shown in Fig. 3(b)). The LEBS peak forms at the

#169818 - $15.00 USD Received 6 Jun 2012; revised 3 Aug 2012; accepted 6 Aug 2012; published 13 Aug 2012

plane of the illumination fiber. As shown in Figs. 3(b) and 6, the probe (assembled by OFS Fitel, Specialty Photonics Division, Avon, CT) is comprised of 4 adjacent optical fibers (each fiber being glass/glass/polyimide/acrylate 50/60/70/160μm diameter,0.22 NA) and a BK7 glass rod (length = 9 ± 0.1mm, refractive index = 1.51).

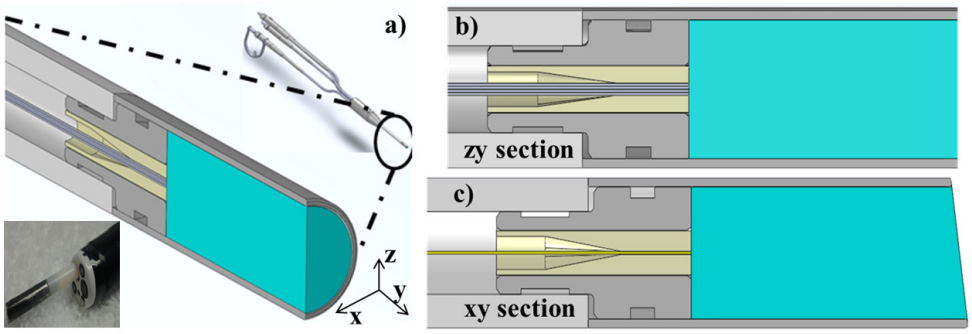

Fig. 6. (a) Depiction of an LEBS fiber optic probe configuration (length is shortened for illustrative purposes), with enlarged cross-section represented. The glass rod (green) is attached to the glass ferrule (yellow) containing four fibers arranged collinearly via an index-matched epoxy. Left inset shows an actual picture of the probe coming out from accessory channel of endoscope. (b) & (c) show the zy and xy cross sections, respectively, of the probe.

The fibers (Polymicro Tech., AZ) are arranged in a linear array (Fig. 6(b)) within a custom extruded glass ferrule (Fig. 6(b) yellow), cemented together, and polished flat on the aligned fiber end faces. The buffer and jacket are removed from the fiber ends (within the glass ferrule) prior to installation in order to provide a 60 ± 3 μm nominal center-to-center spacing. In order to reduce specular reflections, the distal tip of the glass rod is beveled to 9.5°.

The average penetration depth, as well as the measurement of backscattering intensity cones, is governed by the selection of L_{SC} [14]. It is therefore necessary to control L_{SC} to obtain depth selectivity. According to the Van Cittert-Zernike theorem [18] the spatial coherence length (L_{SC}) of

$$Lsc = \frac{\lambda l}{2\pi m} \tag{7}$$

light can be tuned by setting the core radius of the fibers (r), length of the glass rod (l), or refractive index of the glass rod (n). The illumination fiber was coupled to a 35W Xenon lamp (HPX 2000, Ocean Optics, FL) and the three collection fibers were coupled to 3 miniature fiber spectrometers (USB 2000 + , Ocean Optics, FL). Component tolerances were tightly controlled during fabrication, and experimental verification confirmed that the desired L_{SC} attained in assembled probes was achieved. To this end, the spatial coherence function $C(r)$ was obtained via measurement of the angular intensity distribution by illuminating each fiber with light and imaging the fiber onto the CCD camera (Fig. 7(a)) (Excelon, Princeton Instruments, NJ). According to the Van Cittert-Zernike theorem [6, 18], $C(r)$ is the normalized Fourier transform of the angular intensity distribution of the source. The incoherent light emitted by the fiber gains spatial coherence as it propagates through the glass rod. Assuming a perfectly circular source intensity distribution, the $C(r)$ of the light is given by Eq. (8). Where J_1 is a first-order Bessel function of the first kind. As shown in Fig. 7(b), close agreement (R^2~0.9) between the theoretical $C(r)$ given by Eq. (8) and the experimentally measured $C(r)$ at 680 nm is seen. The lesser oscillations in the experiment are possibly due to the fact that an ideal top hat profile is not obtained which dampens these oscillations.

#169818 - $15.00 USD Received 6 Jun 2012; revised 3 Aug 2012; accepted 6 Aug 2012; published 13 Aug 2012

$$C(r) = \frac{2J_1(\frac{r}{L_{sc}})}{(\frac{r}{L_{sc}})} \tag{8}$$

The experimentally measured L_{SC} was determined to be ~27µm, which matches the L_{SC} calculated by Eq. (7). It should be noted that the probe needs to be used in contact mode to attain this L_{SC}.

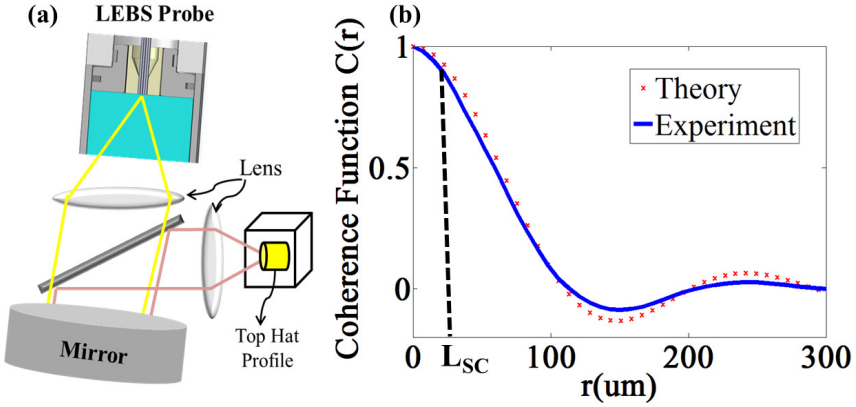

Fig. 7. (a) The setup used for measurement of C(r) of the source (Z) channel of the LEBS probe (b) The experimentally observed C(r) from the LEBS probe corresponds very well with theoretical C(r) from Eq. (2) confirming an L_{SC} of 27µm for the probe. (2)

Since a lens is absent, the beam has an L_{SC} of 27 µm at the tip (maintained by the length of the glass rod). The beam diverges after that point and the resultant L_{SC} changes accordingly. Apart from the current design we have successfully implemented Lsc of 43um (r = 25um, l = 15, outer diameter = 5mm) and could find off the shelf components to implement the probe with L_{sc} upto 86um (r = 12.5um, l = 15, outer diameter = 5mm).

5. Validation of LEBS measurement by phantom and Monte Carlo simulations

In sections 2, 3 and 4 we showed the principles, feasibility and design of converting the LEBS *ex-vivo* system into a fiber optic probe with a capability of *in-vivo* measurement. In this section we want to experimentally verify our claim as to the capability of building a probe based on the principle of collecting three backscattering intensity cones to measure μ_s* with LEBS. In order to verify this claim, we performed an experiment with a phantom (which mimics the optical properties of tissues) of varying μ_s* with constant g. The phantom was prepared by mixing polystyrene beads (Thermo Fisher, CT) in water to attain certain μ_s* & g (the mixing ratios were determined by Mie theory).The readings of LEBS intensities were obtained by measurement of these phantoms with the lens-free fiber optic probe. The choice of the polystyrene bead phantoms is attractive since their scattering behavior is governed by Mie theory and our group has developed Mie Monte Carlo simulations for simulating the LEBS peak obtained in 2D from these phantoms [16,18]. These 2D LEBS peaks obtained from Mie MC Simulations have been validated [16, 18] by matching them to experimentally observed 2D peaks from *ex-vivo* systems.

Hence, the LEBS intensities measured experimentally from the fiber optic probe can be matched with the MC simulation by analyzing the same angles as collected by the probe. This will provide the gold standard test for verifying whether the probe measures LEBS. We measured the LEBS interference intensity $E(\Theta = 0.6°, \lambda)$, which is defined in Eq. (5) as the I_A-

#169818 - $15.00 USD Received 6 Jun 2012; revised 3 Aug 2012; accepted 6 Aug 2012; published 13 Aug 2012

I_B (obtained after background subtraction and normalization by a spectralon reflectance standard with >98% reflectance).

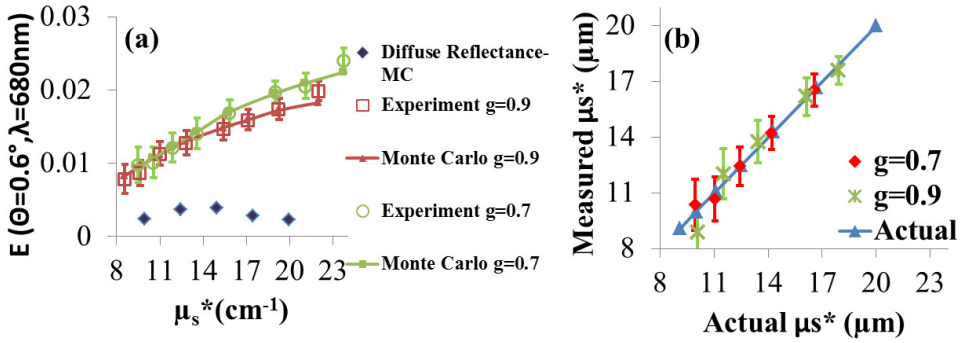

Fig. 8. (a) The experimental LEBS intensity (E(Θ,λ)) for a lens-free probe matches closely (r2~0.9) with interference (LEBS) MC simulation. The LEBS intensity shows a significant residual signal (IA-IB) from interference which is directly proportional to μs* while, diffuse reflectance (DR) MC signal is close to zero with no dependence on μs*.(b)An independent validation curve where the μs* measured from phantoms of prescribed optical properties by the probe shows excellent agreement (R2~0.99).

This ensures that only enhanced backscattering intensity is isolated, since the raw intensity from the probe has LEBS and diffuse components in every channel (Eq. (2) and (3)), and after subtraction the diffuse component which is equal in both is eliminated (Eq. (4) and (5)). The values of this parameter $E(\Theta = 0.6°,680nm)$ were matched with results from the Monte Carlo (MC) simulation method based on Mie theory for LEBS discussed in other publications [6] and section 3. To calculate $E(\Theta = 0.6°,680nm)$ from MC, we superimposed the collection geometry of the probe on the 2D LEBS peak to measure angles corresponding to collection fibers for varying μ_s* & g as shown in Fig. 4(a). From this MC result we calculated $E(\Theta = 0.6°,680nm)$ from Eq. (5) (as I_A-I_B) and matched it with experimental data obtained from the probe. As shown in Fig. 8(a), there is a good match (R^2~0.9) between the MC and experimental data after applying a constant multiplicative scaling factor as described in our previous publications [6,16].

In addition the corresponding diffuse reflectance signal (DR) defined in Eq. (9) is also

$$DR = I_{Diffuse}(\Theta = \pm 0.6°, \lambda) - I_{Diffuse}(\Theta = 1.18°, \lambda) \quad (9)$$

shown in Fig. 8(a). It can be seen that this intensity is close to zero, indicating the absence of enhanced intensity along with showing no trend (proportionality) with μ_s*. This set of data (Fig. 8(a)) has three implications: first, that that the probe experimentally measures an LEBS signal which matches with the *ex-vivo* setup and MC simulations; second, that $E(\Theta = 0.6°)$ can be used to extract μ_s* by using a lookup table; and third, the diffuse reflectance signal ($I_{Diffuse}(A)$- $I_{Diffuse}(B)$) obtained from the MC simulation of our probe has flat dependency with μ_s*, the value of which is close to zero (not measuring the enhanced intensity signal and hence μ_s*). To extract μ_s* from $E(\Theta = 0.6°,680nm)$ we constructed a lookup table by using MC data and validated the measured optical properties with actual optical properties from an independent set of phantoms. As shown in Fig. 8(b), there is a good match between actual μ_s* and μ_s* measured by the probe (R^2~0.9). Subsequently, fractal dimension (D_f) can be calculated by using the dependence of μ_s* with λ as described in [5] and is given by Eq. (10) as:

#169818 - $15.00 USD Received 6 Jun 2012; revised 3 Aug 2012; accepted 6 Aug 2012; published 13 Aug 2012

$$D_f = \frac{dE(\Theta = 0.6°, \lambda) * \lambda c}{d\lambda * E(\Theta = 0.6°, \lambda c} * 0.4 + 1.54 \quad (10)$$

where, λ_c is the central (average) wavelength.

6. Demonstration of depth-limited measurement

Although in previous sections we have shown the ability of the LEBS probe to accurately measure scattering optical properties, it is also important to achieve depth selectivity, as the location of abnormal tissue in precancer is limited to the topmost mucosal layer. For example, it is known that epithelial cells which are located at the bottom of the colon crypt can accumulate mutations over a period of years and thus are the initiating cells in colon carcinogenesis [3]. It is therefore crucial to have the ability to optimally probe these changes with a depth-limited measurement. Depth selectivity is an inherent advantage of LEBS, since the LEBS peak is obtained by combining the EBS measurements with low spatial coherence and broadband illumination. In our previous studies [14], we showed that low spatial coherence illumination ($L_{sc} < ls << ls^*$) behaves as a spatial filter that rejects longer path lengths. Therefore, the penetration depth of LEBS photons can be limited by restricting the spatial coherence length of illumination, L_{sc}.

The depth dependence of the LEBS enhancement for the 2D peak has been well characterized [14] and can be easily applied to probe geometry. We wanted to verify and characterize the dependency of optical scattering properties measured by the probe with an average penetration depth. For a given optical property, a saturation curve C(T)

$$C(T) = \int_o^T p(Z)dZ \quad (11)$$

(where p(Z) is the probability that light returns from depth Z was constructed for $E(\Theta = 0.6°, 680nm)$ by limiting the maximum depth from which rays were reflected (by modifying the thickness of medium via post-processing of MC data) [14]. The normalized derivative (p(Z) = dC/dT) of the saturation curve yielded the probability distribution as a function of depth, p(Z). The average penetration depth (PD_{avg}) was then calculated according to the first moment [14]:

$$PD_{avg} = \int zp(Z)dz \quad (12)$$

Empirically, the average penetration depth (Eq. (12)) can be represented in closed form as:

$$PD_{avg} = a(L_{SC})^{1-b}(ls^*)^b \quad (13)$$

Where:

$$\begin{aligned} a &= a_0 + a_1 g + a_2 g^2 \\ b &= b_0 + b_1 (1-g)^{b_2} \end{aligned} \quad (14)$$

The term a and the power b depend on the anisotropy factor g (as described by Eq. (14)). The constants are $a_0 = 0.54$, $a_1 = -0.11$, $a_2 = -0.23$, $b_0 = 0.79$, $b_1 = 0.24$, and $b_2 = 0.75$. The expressions in Eq. (13) and values of the coefficients are obtained empirically by fitting with Monte Carlo simulations. For tissue g~0.9 (which yields a = 0.26 & b = 0.84), the resultant average penetration depth for the probe is 116μm (with $ls^* = 800$). As shown in Eq. (13), the average penetration depth of the probe is directly proportional to L_{SC} and can be limited (by modifying probe geometry) to the required range based on the application. We validated the accuracy of the equation for a range of ls^* and g relevant to a tissue regime by comparing the

#169818 - $15.00 USD Received 6 Jun 2012; revised 3 Aug 2012; accepted 6 Aug 2012; published 13 Aug 2012

values of average penetration depth obtained from the equation with MC simulations at L_{SC} = 27 µm. As shown in Fig. 9, good agreement (R^2~0.99) is achieved between the two suggesting the validity of the derived equation.

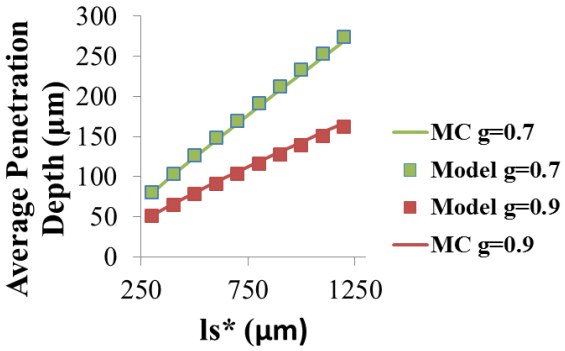

Fig. 9. The validity of Eq. (13) is verified by comparing the average penetration depth (L_{SC} = 27 µm) with the simulation using Mie theory phase function [14]. Good agreement (R^2~0.99) is achieved between both indicating validity of the equation.

In order to experimentally verify the claim of depth-limited detection of μ_s*, we carried out an experiment with a two-layered phantom. The two-layered tissue phantoms consisted of a thin superficial layer and a basal layer (Fig. 10(a)). The thin superficial layer was composed of a suspension of polystyrene microspheres and did not contain Hemoglobin (Hb) to mimic the epithelial layer. The basal layer consisted of a suspension of polystyrene microspheres to mimic tissue scattering and Hb to mimic light absorption in tissue. In cases where the top epithelial layer is thin, the photons contributing to the LEBS signal penetrate through the top layer into the basal layer and have a peculiar Hb absorption band at 540nm. In other scenarios where the top layer is thick, all LEBS photons are localized in the top layer and the signal does not depict an Hb absorption band. This methodology allowed us to experimentally validate a probe average penetration of around 116 µm. In order to perform this experiment we varied the thickness of the top layer from 0 µm to 65 µm and 130 µm while keeping the basal layer the same. The basal layer was prepared as a solid phantom consisting of the suspension of 4.3 µm polystyrene microspheres, agarose (2%) and Human Hemoglobin. The concentrations were controlled appropriately to give ls* of 500 µm, g = 0.9, [Hb] = 10.4g/L and the thickness was controlled to 5mm. The optical properties of the basal layer closely resemble those of human biological tissue. The thin superficial layer was made as a solid phantom slab consisting of the suspension of polystyrene microspheres of 0.87 µm (with no Hb) and the optical properties were set to be ls* = 800 µm and g = 0.9, mimicking the epithelial layer. The desired thickness was achieved by pouring this suspension in mold with a spacer of particular thickness and allowing it to solidify followed by subsequent removal. To perform the experiments, the thin slabs were placed on a solid medium and the readings were taken from the probe placed in contact with a top layer of varying thickness. As shown in Fig. 10(b) the LEBS intensity spectra at a thickness of zero (Ts = 0µm, no top layer) shows the strongest absorption band, indicating all photons traveling in the basal layer. In cases where thickness is 65µm the absorption band is muted, followed by disappearance when the thickness is increased to 130µm (exceeding the average penetration depth of the LEBS probe as calculated by Eq. (13)). This indicates that at 130 µm almost all the photons are localized within the top layer, which highlights one important aspect of the depth selectivity of the probe.

#169818 - $15.00 USD Received 6 Jun 2012; revised 3 Aug 2012; accepted 6 Aug 2012; published 13 Aug 2012

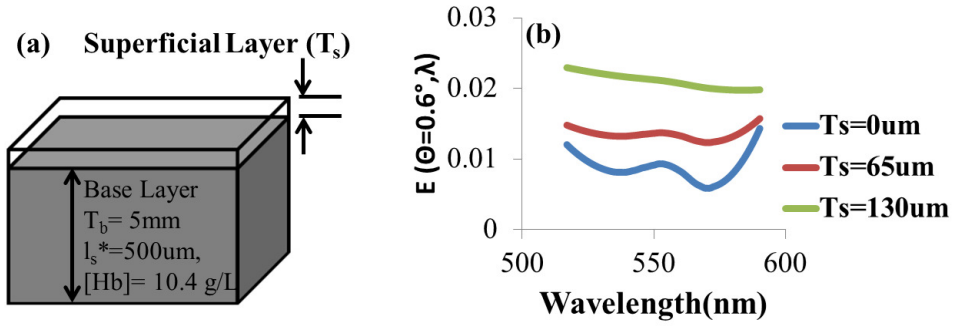

Fig. 10. (a) Schematic of a two-layered phantom. The phantom consists of a superficial layer of thickness Ts and a basal layer of thickness TB. The basal layer is made of scatterers and Hb. The superficial layer is made only of scatterers but no absorber. (b) Shows a representative LEBS intensity spectrum for various superficial layer thicknesses. As the thickness is increased the absorption band vanishes, indicating a localization of LEBS photons to the top 130 microns.

7. Discussion

The majority of precancerous structural changes occur in the mucosal layer [2,3]. These structural changes can be quantified by measuring changes in the depth-limited optical properties of this layer. LEBS is an attractive technique due to its ability to measure depth-resolved optical properties with sensitivity to sub-diffusion length scales. In our recent publications we have shown in *ex-vivo* studies that measurements of optical properties by LEBS in the rectal mucosal biopsies were able to predict the risk of cancer being present elsewhere in the colon with 90% accuracy (area under ROC curve) [7]. With the aim of translating this technique for *in-vivo* application, we have presented the design and implementation of a lens-free fiber-optic LEBS probe. The design was based on using the symmetric properties of the LEBS peak to obtain selective angular intensities from the LEBS peak cone to interpret and calculate depth-limited optical properties. Based on measurements obtained from phantoms and MC simulation of the probe, we are able to achieve agreement between experimentally observed and theoretically predicted LEBS parameters and optical properties (Fig. 8). The claim of depth selectivity (top 120 µm) is verified with MC simulations and two-layered phantom experiments (Fig. 9 and 10).

The probe configuration seems very similar to that seen for a number of diffuse reflectance probes which contain a delivery fiber and one or more collection fibers with the addition of a spacer [8–11]. However, the novelty in our probe lies in fact that it is the first demonstration of the measurement of enhanced intensity (LEBS) in the backward direction over and above the diffuse intensity (Fig. 4, 5, and 8). The LEBS detection is advantageous since it provides a capability for depth-limited measurement of optical properties along with sensitivity to sub-diffusion length scales. The other probe geometries using diffuse reflectance (DR) or differential path length spectroscopy (DPLS) which utilize a similar geometry to our probe cannot achieve the measurement of enhanced backscattering (LEBS) for two reasons: 1) absence of finite spatial coherence (L_{SC}) and 2) the absence of close spacing between different fibers to detect small backscattering angles. The other probe geometries use larger fiber core diameters (above 100µm), which indicates that L_{SC} achieved by these configurations is minimal (from Eq. (1)) resulting in the absence of LEBS. An additional consequence of the larger core diameter is that the collection fibers which are collinear with the source have higher separation, ensuring the collection of angles where the LEBS peak rolls off into the incoherent baseline (diffuse background). Hence, the current probe configurations for DR spectroscopy or DPLS (despite a similar look) cannot measure LEBS (as shown in Fig. 8(a)). In order to overcome these challenges, we employed a fiber with a

#169818 - $15.00 USD Received 6 Jun 2012; revised 3 Aug 2012; accepted 6 Aug 2012; published 13 Aug 2012

core diameter of 50µm and developed a process using a custom fabricated glass ferrule, and stripped the fiber buffer jacket to ensure inter-fiber separation of ~60 µm. This ensured that we met the conditions required for the observation of LEBS (finite L_{SC}) and with fibers at close angles

Conversion of any *ex-vivo* optical modality to an *in-vivo* fiber optic probe involves several considerations and tradeoffs, and may involve some loss of information. In our case we desired the probe to be easy to manufacture in large quantities, inexpensive, and to provide depth-limited information about optical properties of the tissue. In a conventional *ex-vivo* LEBS setup we measure four LEBS parameters (Enhancement (rise of peak above baseline at $\Theta = 0°$), FWHM (full width at half maximum of the peak), spectral slope (Enhancement as a function of wavelength) and fractal dimension (D_f)) from which we obtain optical properties (μ_s*, g & D_f) and physical properties (Δn^2, lc, D_f) via lookup Table [6]. In the case of the lens-free fiber optic probe we had to make compromises due to issues with size, feasibility of implementation *in-vivo*, number of detectors, cost etc., and hence could not measure some of the parameters except for μ_s*(demonstrated in Fig. 8) and D_f (Eq. (10)).Therefore, with the current configuration of the probe, we were only able to measure two (μ_s* & D_f) out of three optical properties (μ_s*, g & D_f) which are measured by the *ex-vivo* system (Fig. 1(a & b)). The reduction of the 2D LEBS peak to three discrete pixels does represent a major loss of information as compared to the full 2D peak, but as demonstrated we only lose information about one optical property (g) with this implementation. Thus, although the $P(r)$ obtained from the *ex-vivo* LEBS system has sensitivity to sub-diffusion light transport length scales for which information about scattering phase function is preserved, this is not realized in the current probe configuration. The sensitivity and measurement of g can only be achieved by either the collection of one more scattering angle (preferably a Z source fiber with beam splitter), sampling the peak with a more closely spaced fiber/2D array, or by making assumptions about phase function. We are currently working on implementing this capability in the second generation of this probe. However, the other two parameters μ_s* & D_f can be reliably extracted as demonstrated here. It is also to be noted that once the probe is assembled the L_{SC} (and subsequent average penetration depth) is fixed and cannot be changed. In the case of the *ex-vivo* LEBS system, L_{SC} can be changed online resulting in the ability for depth-resolved measurement. However, we plan to carry out *ex-vivo* biopsy studies of every relevant organ with the *ex-vivo* system with varying L_{SC} to determine the L_{SC} that gives the best diagnostic differentiation, and then use that L_{SC} to build a fiber optic probe for *in-vivo* use, hence avoiding the limitations we face due to these shortcomings.

8. Conclusion

In summary, we demonstrate the ability to perform depth-limited measurements of reduced scattering coefficient and fractal dimension with a simple fiber optic probe using LEBS. The novelty of the probe research is demonstrated by the first observation of LEBS with a specially engineered lens-free fiber optic probe. The probe is based on the simple concept of discretizing a 2D LEBS peak into a few backscattering angles and then collecting these specific LEBS intensity cones to calculate the optical scattering properties. Depth selectivity is obtained by tuning L_{SC} and is demonstrated with two-layer phantoms and MC simulations. We believe this probe will find applications in material characterization, cancer screening, etc. Further studies in animals and humans are being performed to validate this claim.

Acknowledgment

This work supported by NIH R01CA128641, R01EB003682, R01CA156186 and NSF CBET-0937987 grants. NNM thanks Benjamin Keane for excellent document preparation.

#169818 - $15.00 USD Received 6 Jun 2012; revised 3 Aug 2012; accepted 6 Aug 2012; published 13 Aug 2012